Cardiac Contractility

Fotios G. Pitoulis and Pieter P. de Tombe

C. Terracciano, S. Guymer (eds.), *Heart of the Matter*, Learning Materials in Biosciences,
https://doi.org/10.1007/978-3-030-24219-0_10

What You Will Learn in This Chapter

This chapter will equip you with an understanding of the determinants of cardiac contractility and the changes observed in these within the context of heart failure. We will begin by discussing the fundamentals of cardiac output, the effects of preload and afterload on ventricular function, and their clinical significance.

Learning Objectives

- Understand the main determinants of cardiac performance.
- Appreciate the difference between preload, afterload and contractile state.
- Appreciate the importance of pressure–volume loops.

10.1 What We Know: Cardiac Output

Cardiac output (CO) refers to the volume of blood ejected by the heart in 1 minute, expressed in litres per minute (l/min). CO continuously fluctuates to meet the changing energetic demands of the body and is determined by the product of the stroke volume(SV)(the volume of blood ejected by the heart in each beat) and heart rate (HR), in the following relationship: CO = SV × HR (Eq. 1) [1]. In the first part of this chapter, we will look into the fundamental role of HR in the regulation of CO, and appreciate how SV is governed by preload, afterload and cardiac contractility. The relationship of these parameters in the context of pressure–volume loops will then be discussed.

In response to stress (e.g. exercise, pregnancy, heart failure), a primitive fight-or-flight response is mounted by the adrenergic system, triggering an increase in CO. This is achieved in part through an increase in HR (known as positive chronotropy). Yet, because HR and SV are not independent variables, the effect of HR on CO is not straightforward. In fact, increasing HR decreases SV (Fig. 10.1a). In open-chested dogs, artificially pacing the heart to high HRs causes the CO to increase, reach a plateau and then drop above a threshold value (Fig. 10.1b) [2]. However, the main determinant of CO is venous return and not HR (see *preload*). Generally, maximal CO is expected to occur with the highest possible HR that does not compromise filling [3].

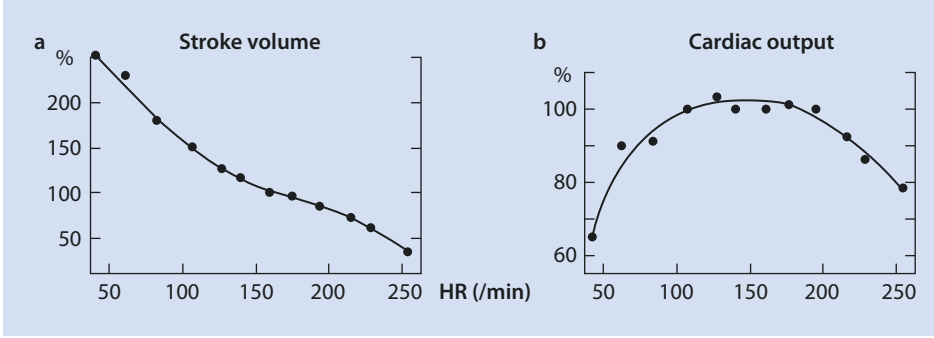

Fig. 10.1 **a** Relationship between SV and HR, and **b** relationship between CO and HR in open-chest canines. (Adapted from [2])

10.1.1 The Role of Ca^{2+} in Cardiac Contraction

During the cardiac action potential, Ca^{2+} influx via sarcolemmal L-type Ca^{2+}-channels leads to Ca^{2+} release from the sarcoplasmic reticulum and the generation of the whole-cell Ca^{2+} transient (see chapter *excitation–contraction coupling*). The subsequent rise in Ca^{2+} then triggers a molecular interaction between thin (actin) and thick (myosin) myofilaments on sarcomeres, the cardiomyocyte's contractile units [4]. The magnitude of force generated by cardiomyocytes is strongly paired to the intracellular Ca^{2+} concentration, $[Ca^{2+}]_i$ [5].

Specifically, increasing $[Ca^{2+}]_i$ results in a non-linear increase in force, meaning that small changes in $[Ca^{2+}]_i$ can result in functionally significant changes in CO [6]. This steep relationship between $[Ca^{2+}]_i$ and force can be described with a negative logarithmic $[Ca^{2+}]_i$ scale (pCa), characterized by a sigmoid curve organized symmetrically around the half-maximum force at pCa_{50}, as shown in Fig. 10.2 [6]. Changes in the sarcomere's myofilament Ca^{2+} sensitivity can affect the magnitude of force generated at a given $[Ca^{2+}]_i$. Interventions that affect myofilament Ca^{2+} sensitivity can shift the curve to the left or right, leading to greater or lesser force generation at a given $[Ca^{2+}]_i$, respectively [7, 8]. For example, decreased pH increases pCa_{50} (decreases Ca^{2+} sensitivity), whereas increasing sarcomere length decreases pCa_{50}, thereby increasing Ca^{2+} sensitivity.

10.1.2 Preload

In 1884, Howell and Donaldson demonstrated that increasing the venous return in an isolated mammalian heart–lung preparation increased CO, whilst decreasing it had the opposite effect [7]. A few years later, Otto Frank and Ernest Starling showed that stepwise increases in diastolic volume and pressure increased the magnitude of cardiac contraction [9, 10]. To study these observations *in vitro*, strips of ventricular myocardium are stretched

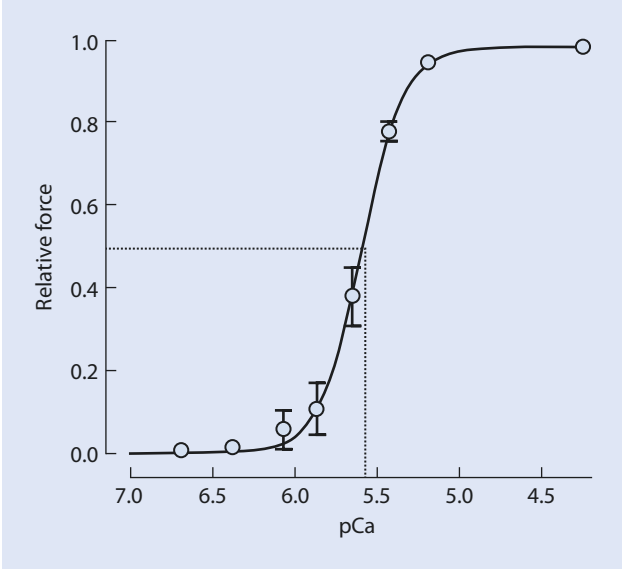

Fig. 10.2 Force–pCa curve in demembranated ventricular preparations where force has a sigmoidal relationship with $[Ca^{2+}]_i$. Dotted lines correspond to pCa_{50}: the $[Ca^{2+}]_i$ at half-maximal force. pCa_{50} is a measure of Ca^{2+} myofilament sensitivity. Decreasing pCa_{50} corresponds to a rightward shift of the curve and a decrease in Ca^{2+} sensitivity. (Modified from Sun et al. [6])

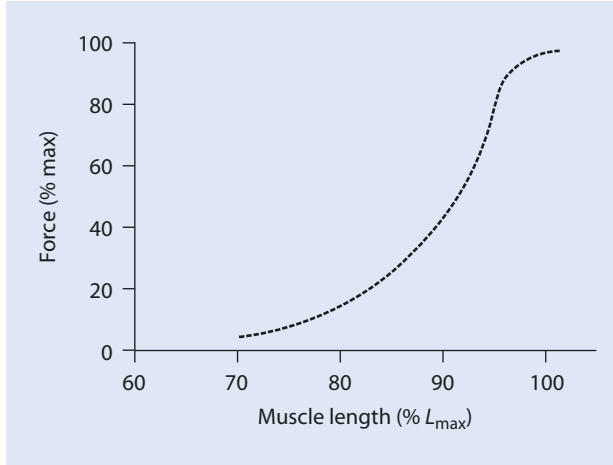

Fig. 10.3 Muscle length–force relationship in cardiac muscle. Increasing muscle length (and consequently sarcomere length) increases force. Notice steepness of relationship. At 70% of L_{max} force tends towards abscissa. Adapted from [10])

to different lengths and the generated force measured. Application of stretch represents a load on the myocardium, termed *preload*. With electrical stimulation, the myocardium contracts, allowing us to investigate the effects of varying preload on contraction. *Increasing preload increases force generation.* This observation is known as force–length relationship or *Frank–Starling Law* (Fig. 10.3).

At the level of the whole heart, increased preload is represented by greater blood filling of the ventricle, increasing end-diastolic volume (EDV) and thus pressure (EDP). This stretches the myocardium, explaining why increased venous return augments cardiac contraction [8]. So, what is the mechanism behind this phenomenon?

Laser diffraction measurements show that at higher preload, sarcomeres in cardiomyocytes are lengthened [8]. When force is plotted as a function of sarcomere length (SL), increasing the latter results in increase in force [9]. The first mechanism to explain this is known as *filament overlap and interference* [9]. *In vivo*, cardiomyocyte SL ranges from 1.8 to 2.2 μm, with maximum force attained at SL 2.2–2.4 μm [11, 13]. At low SLs (<2.0 μm), thin filaments cross the midline, extending into the 'wrong' half of the sarcomere. This leads to a fraction of myosin heads pulling in the opposite direction, hampering net force production [8]. Stretching the sarcomeres minimizes this interference, increasing contractile performance [11, 14]. Although this partly explains the ascending limb of the force–length relationship (Fig. 10.3), other physical mechanisms such as opposing forces due to compression of the thick filaments at the Z-bands at low muscle lengths have been proposed to explain the steep part of the force–length function [10].

However, by far the most important mechanism underlying the Frank–Starling law is the dynamic relationship between SL and myofilament Ca^{2+} sensitivity [5]. Increasing SL increases myofilament Ca^{2+} sensitivity, leading to a leftward shift in the force–Ca^{2+} curve and an immediately increased contraction at any given $[Ca^{2+}]_i$, shown in Fig. 10.4 [7, 11, 15]. An increase in SL also causes a delayed increase in the amplitude of the Ca^{2+} transient. The latter accounts for ≈30% of the total force increase observed with stretch [12].

Thus, we have seen that an increase in preload increases force generation in a biphasic manner, namely, with an immediate component, that is, the shift in Ca^{2+}myofilament sensitivity, and a delayed component, namely, the increase in Ca^{2+} transient amplitude. It is generally agreed that the Frank–Starling law refers to the immediate component, and this will be the focus of the following discussion.

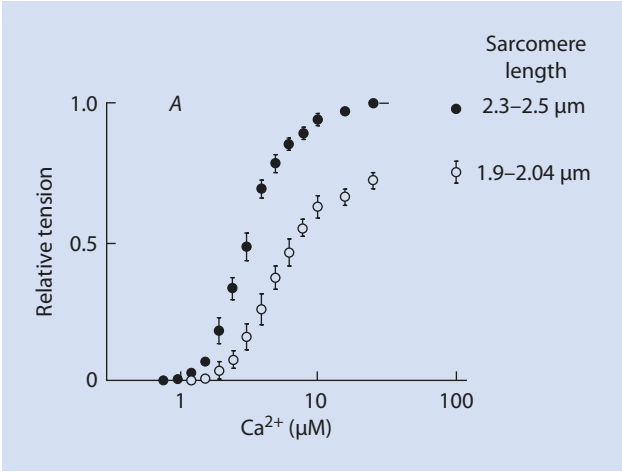

Fig. 10.4 Force-Ca^{2+} Curve. Increasing Ca^{2+} concentration increases force generation in a non-linear manner. Increasing sarcomere length (i.e. increasing preload) from 1.9–2.04 µm to 2.3–2.5 µm increases the myofilament Ca^{2+} sensitivity leading to greater force at any given Ca^{2+}. (Adapted from Hibberd et al. [32])

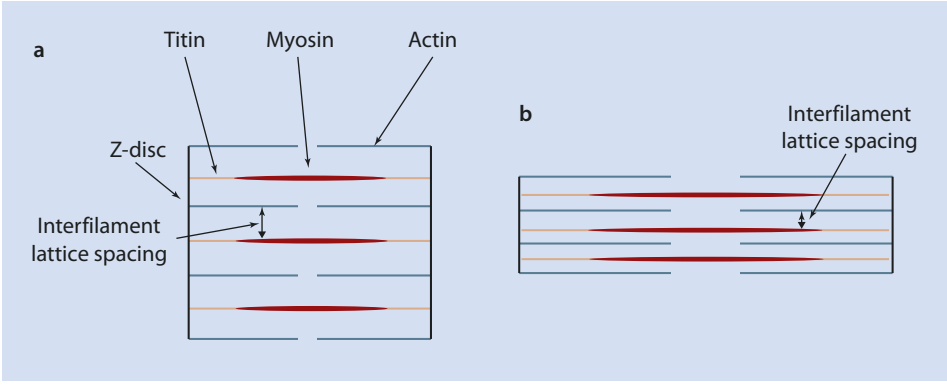

Fig. 10.5 Interfilament lattice spacing theory of length-dependent activation. For a cross-bridge cycle to occur, myosin heads must bind to myosin binding sites on actin. According to the interfilament lattice spacing theory, when sarcomeres are stretched (from **a** to **b**), the distance between myosin and actin decreases, promoting the cross-bridge cycle and the generation of force

This leaves us with the task of explaining the increased myofilament Ca^{2+} sensitivity at increased SLs. One hypothesis is that increasing SL decreases interfilament lattice spacing. As the volume of a cardiomyocyte is constant, increases in length are accompanied by a decrease in the spacing between subcellular components, such as the distance between filaments in the sarcomeres. This enhances the probability of an interaction between thick and thin filaments, thereby increasing force generation at a given $[Ca^{2+}]_i$ as illustrated in Fig. 10.5 [13].

The interfilament lattice space theory may be insufficient to explain the length-dependent increase in myofilament sensitivity on its own. X-ray diffraction patterns suggest that increasing SL results in a superior orientation of myosin heads on the thick filament backbone, which may contribute to the increase in force [14].

We have therefore seen that the muscle length–force relationship is a consequence of 'physical' and 'activating' factors [10]. The former refers to changes in myofilament overlap and opposing forces with muscle length changes, whereas the latter refers to changes in myofilament sensitivity to Ca^{2+}. Overall, increased preload leads to increased force gen-

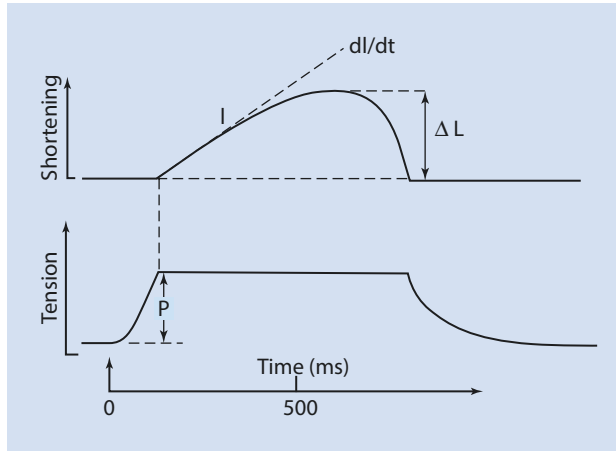

Fig. 10.6 Tracing of an isolated cat papillary muscle shortening in the presence of afterload. Following electrical stimulation (time point 0), the muscle begins to develop force (tension). As the force approximates the afterload, the muscle is able to pull the load and thus shorten. Note that the muscle is lifting both preload and afterload (*P*). Shortening is represented by ΔL, whilst *dl/dt* is the first derivative of shortening (i.e. velocity of shortening), highest at the beginning of contraction. (Adapted from Sonneblick et al. [15])

eration by the myocardium. In the normal heart, preload is established by the diastolic filling of the ventricles (represented by EDP or EDV), which serves to determine the subsequent magnitude of contraction. With greater blood filling, myocardial fibre stretch increases, leading to an increased SV and CO.

10.1.3 Afterload

Another determinant of cardiac performance is *afterload*, defined as the mechanical load imposed on the ventricle during the ejection phase. At the level of the whole heart, afterload is broadly represented by the aortic pressure, that is, the pressure the ventricles must produce to eject blood into the aorta [1]. Once ventricular pressure exceeds aortic pressure, the aortic valve opens to facilitate the propulsion of blood into the circulation [9]. At the cardiomyocyte level, once the developed force starts approximating the afterload, sarcomeres begin to shorten and contraction shifts from isometric (constant length) to isotonic (changing length), as shown in Fig. 10.6 [15].

As we previously described, preload can be applied on isolated ventricular strips by stretching the tissue, typically done by hanging weights on the preparation. In more complex experimental setups (utilizing a stop lever), weights can be added such that they will only be encountered once the muscle starts contracting, that is, representing the afterload. Thus, before the beginning of contraction, the muscle is stretched by the preload; however, after the onset of contraction, the muscle will lift both the preload and afterload, with total lifted load $P = preload + afterload$ [15]. If cardiac performance is defined as the mechanical work performed by the muscle, then:

$$\text{Work} = P \times \Delta L$$

where ΔL is the total shortening of the myocardium.

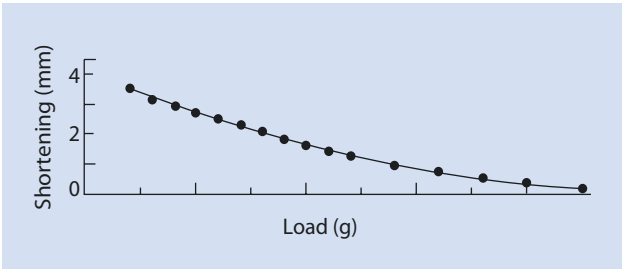

Fig. 10.7 Effect of afterload on shortening of isolated cat papillary muscles. (Adapted from Sonneblick et al. [15])

By varying preload and afterload, their influence on cardiac performance can be deciphered. The first observation is that for a given preload, increasing afterload diminishes ΔL in a monotonic function due to the muscle contracting against greater resistance. Eventually, the muscle is unable to pull the load (i.e. it cannot shorten; isometric contraction), as shown in Fig. 10.7 [19–21]. Therefore, when afterload is so high that the muscle is contracting isometrically (i.e. $\Delta L = 0$), $W = 0$. Secondly, if we allow afterload to approach 0, then ΔL will be maximal, as the muscle is shortening against ≈0 resistance; work will also be 0 as $P \approx 0$.

Understanding the role of afterload is important clinically as pharmacological agents and/or mechanical devices may be used to alter it, increasing the myocardial contractile capacity (and thereby CO), whilst decreasing the workload (and by extension energetic demands) on the heart. In general, the more loaded the tissue, the higher the metabolic demands so unloading the heart (e.g. with assist devices) can limit energy and O_2 consumption [16], which is important both acutely (e.g. acute myocardial infarction) and chronically (e.g. heart failure). A completely unloaded left ventricle has an average consumption of 2 ml O_2 per minute per 100 g of muscle [17].

10.1.4 Cardiac Contractility

'*Contractility*' refers to the inotropic capacity of the myocardium and describes the ability of the heart to eject blood at a given preload and afterload [22, 23]. If CO is plotted as a function of left-ventricular end-diastolic pressure (LVEDP), the graph that is obtained is called Frank–Starling or ventricular function curve and shows a curvilinear CO increase with increasing LVEDP [8]. These curves show that for any given LVEDP, an increase in myocardial contractility shifts the curve upwards and to the left (Fig. 10.8).

The principal determinant of the cardiac inotropic state (i.e. contractility) is the autonomic nervous system (ANS). Specifically, the sympathetic arm of the ANS mounts the cardiac adrenergic response via the release of cardiac-acting catecholamines including adrenaline and noradrenaline. The former is synthesized in the adrenal medulla and secreted into the circulation, whilst the latter is released directly into the cardiac interstitium by sympathetic fibres [19]. At the cellular level, adrenergic stimulation regulates the excitation–contraction coupling machinery in the following ways:

1. Increased Ca^{2+} transient amplitude, meaning greater activation of cross-bridges and stronger contraction (positive inotropy).
2. Increased heart rate and accelerated contraction (positive chronotropy).
3. An abbreviation of the Ca^{2+} transient and action potential duration, with a faster relaxation (positive lusitropy).

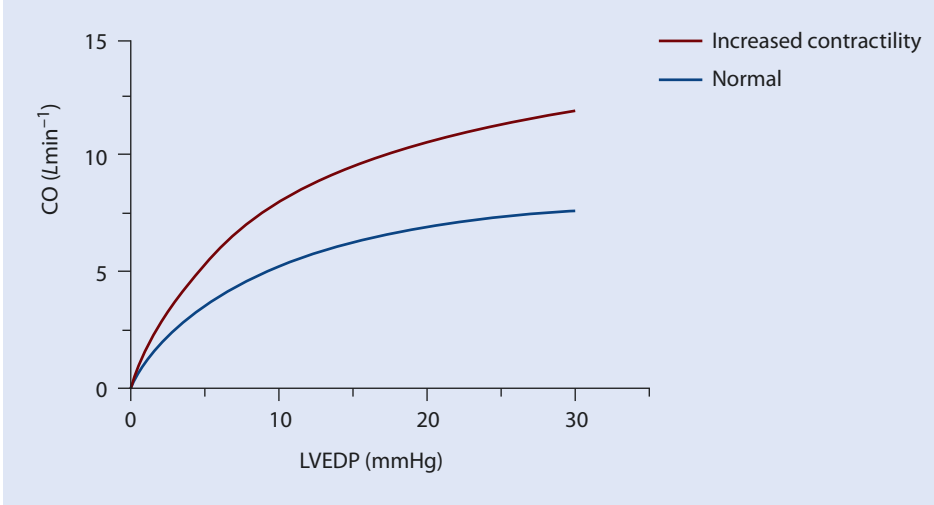

Fig. 10.8 Frank-starling curve at normal and increased contractility. Preload is represented by the LVEDP. Notice that increasing contractility (red curve) increases CO at any given preload

Fluctuations in energetic demands lead to corresponding changes in adrenergic stimulation to maintain the CO. As such, the heart is constantly exposed to varying concentrations of catecholamines, allowing it to operate on a whole spectrum of Frank–Starling curves proportional to the level of adrenergic stimulation.

10.1.5 Pressure–Volume Loops

We will now consider the effect of cardiac performance determinants in the context of pressure–volume (PV) loops. The heart is a pressure generator constantly expending energy to perform mechanical work. As we have seen at the level of ventricular strips or cardiomyocytes, this takes the form of myocyte shortening (ΔL) and force generation. At the level of the heart, mechanical work is best described by changes in ventricular pressure and volume. If a ventricle of area A *(cm^2)* contracts by length L *(cm),* then $L \times A$ represents a change in ventricular volume (ΔV, *cm^3*). As the ventricle is contracting, a force F *is* applied on A, such that F/A represents a change in pressure (ΔP) [8]. When the relationship between pressure and volume is plotted over an entire cardiac cycle, a PV loop is obtained [20].

In PV loops, volume is represented on the *x-axis*, whilst pressure is on the *y-axis*. Each side of the loop represents one phase of the cardiac cycle, drawn in counterclockwise directions beginning with

1. Isovolumetric contraction, whereby ventricular pressure rises at constant volume.
2. Rapid ejection phase, when pressure rises correspondent with a drop in ventricular volume.
3. Isovolumetric relaxation, during which pressure drops at constant volume.
4. Diastolic filling—associated with ventricular filling and small increases in volume and pressure.

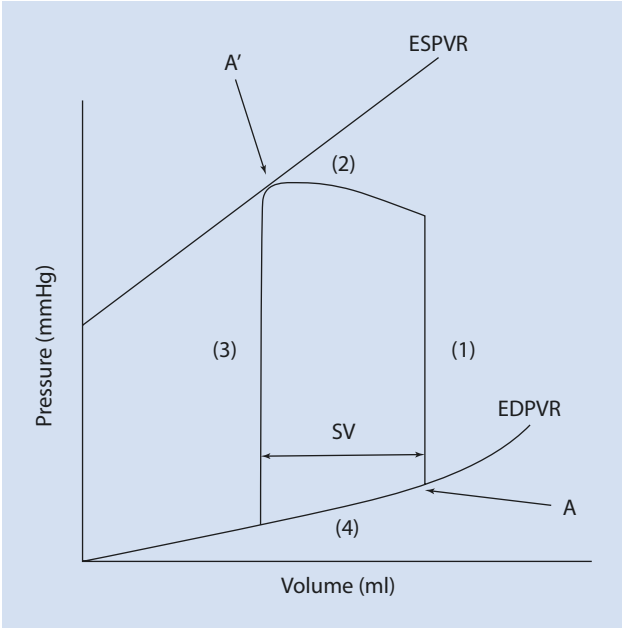

Fig. 10.9 Pressure-Volume Loop. Isovolumic contraction begins at point A, which denotes the end-diastolic volume and pressure. Ejection then follows, with point A′ denoting the end-systolic volume and pressure, followed by isovolumic relaxation. This is followed by diastolic filling. A and A′ are points on the end-diastolic pressure–volume (EDPVR) and end-systolic pressure–volume relationship (ESPVR), respectively

A typical PV loop is shown in Fig. 10.9. Stroke volume can be calculated as the difference between EDV and end-systolic volume (ESV) -that is, $SV = EDV - ESV$. Ejection fraction (EF), a measure of the proportion of blood ejected from EDV, can then be calculated [18] as $EF = SV/EDV$. In a healthy adult, stroke volume is ≈70 ml and EDV ≈ 120 ml, producing an EF of ≈0.58. EF is a measure of the pumping efficiency and is often altered in pathology.

The point on the PV loop just before isovolumic contraction (A) demarcates the end-diastolic volume and pressure, sitting on a given end-diastolic pressure–volume relationship (EDPVR). Likewise, the point at the end of the ejection phase (A') denotes the end-systolic volume and pressure, sitting on the end-systolic pressure–volume relationship (ESPVR). Both EDPVR and ESPVR are important determinants of ventricular function. The EDV determines the stretch on myocardial fibres (and thus preload), with a higher EDV resulting in an increased SV (Fig. 10.10a). The actual position of the EDV on the PV loop is dependent on the EDPVR, which describes the ventricular wall compliance. This can be altered in pathology, meaning that the same EDV may correspond to a different EDP if the EDPVR is altered [20]. As we have seen, a decrease in afterload allows the muscle to shorten more, decreasing ESV and thereby increasing SV for a given EDV (Fig. 10.10b). In the same manner, as we have described the EDV and EDP at end-diastole, the same can be done for end-systole in a relationship known as ESPVR. The ESPVR tells us about the contractile state of the myocardium. Notice that for a change in afterload or preload (Fig. 10.10a, b), the SV and the peak developed pressure (defined as the highest point on the PV loop) change, yet the end-systolic point always 'hits' the ESPVR line.

Thus, changes in loading of the heart (i.e. preload or afterload) may lead to changes in SV or peak pressure but will always end up on the ESPVR. This makes the ESPVR a *load-independent measure of contractility* [21]. In contrast, changes in the contractile state, such

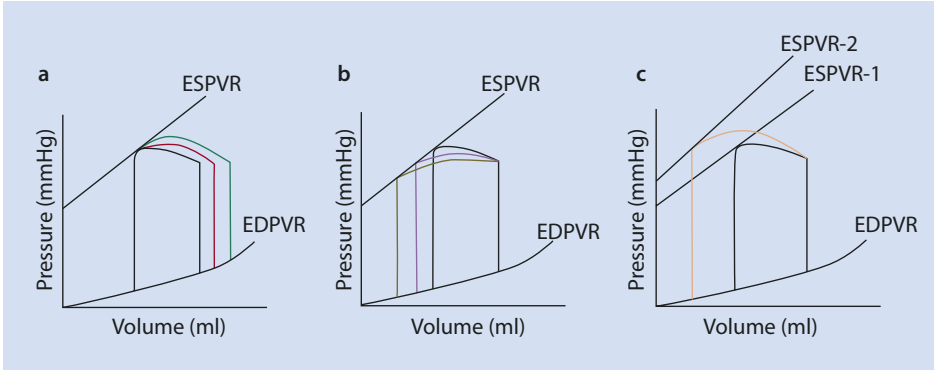

Fig. 10.10 Pressure-Volume loops at different preload, afterload, and inotropic states. **a** Increasing diastolic filling (green>red>black) at a given EDPVR increases the SV. **b** Decreasing afterload at a given EDPVR and ESPVR increases the SV (brown>purple>black). **c** Increasing the inotropic state causes a change in the ESPVR, increasing its slope (orange>black)

as a positive inotropic intervention (e.g. adrenergic stimulation), will change the ESPVR, reflecting a change in the contractile state of the heart (Fig. 10.10c). As the ESPVR is typically fit with a linear regression, the contractile state of the heart can be quantified by the slope of the ESPVR, such that a positive inotropic agent increases the slope, whereas a negative inotropic agent decreases it.

PV loops are the ultimate cardiac biomechanics descriptors, characterizing both the intrinsic properties of the ventricle and the coupling of the latter with the vasculature (e.g. increased afterload due to high blood pressure would shift the shape and height of a given PV loop). Together with technological advancements, they have enabled noninvasive assessment of ventricular properties, with immediate implications for diagnosis, prognosis and treatment of disease [22]. For example, with progressively worsening heart disease profile, it is widely accepted that EF typically falls. However, when an all-encompassing outcome including all-cause mortality, transplantation and mechanical circulatory support device implantation is correlated against PV loop parameters, the best predictor is EDV [23]. Likewise, changes in loop morphology can be used to appreciate ventricular remodelling as seen with progressive heart disease where both the width and the height of PV loops decrease, reflecting decreased SV and pressure generation, respectively [23].

10.2 Clinical Implications

The clinical importance of the regulators of myocardial contractility can be appreciated by investigating what happens when these go erratic. Heart failure (HF) is a variable clinical syndrome manifesting as the convergent endpoint pathway for a variety of pathological processes that impair myocardial function. One such process is arterial hypertension. High blood pressure is the single most important risk factor for HF, and it is estimated that up to 75% of HF cases have had antecedent hypertension [24]. In arterial hypertension, afterload is increased such that the ventricle typically spends a prolonged time in isometric

contraction [25]. At such afterload the amount of work performed by the heart increases. To cope with this increased demand, the heart, being a terminally differentiated organ, enlarges leading to ventricular wall thickening (i.e. hypertrophy). If the pressure overload persists, this initially adaptive hypertrophic mechanism progresses towards maladaptive failure [24, 26]. When pathologically high blood pressure is modelled *in vivo* by chronic aortic band constriction, pathological ventricular remodelling ensues in the form of increased fibrosis, inflammation and apoptosis, coupled with decreased EF and aberrant calcium handling, ultimately progressing to HF [27]. Likewise, when preload is modelled *in vivo* by increasing ventricular volume via vena cava shunting progression to HF follows, yet the underlying pathways are not the same as those activated in response to pressure overload [27].

Pathological remodelling of the heart in response to such abnormal conditions of mechanical overload has been shown to be potentially reversible with the use of mechanical circulatory support devices, known as left-ventricular assist devices (LVADs) [28]. Data suggests that haemodynamic unloading mediates improvements in ventricular function and structure (i.e. 'reverse remodelling') by changes in myocyte size and structure, calcium homeostasis, extracellular matrix and fibrosis, as well as signal transduction pathways [28–30].

10.3 What We Don't Know and Where We are Heading: Isolating Mechanical Load

We have seen the importance of preload, afterload and contractility in determining the performance of the heart, their detrimental effects when they go haywire, as well as the clinical utility of PV loops in the assessment of heart physiology and pathology. However, a complete understanding of the full picture of mechanical loading on the function of the heart is still lacking. Abnormal preload and afterload both converge to heart dysfunction, yet their underlying pathways are not identical [27]. Additionally, although *in vivo* experiments [27] yield valuable information and are the final hurdles to be surpassed to progress to human trials, the haemodynamic system is intrinsically linked to the neurohormonal axis. In response to pressure overload or an injury to the heart, the drop in CO is met by a compensatory rise in the adrenergic system in order to maintain CO [31]. Despite its short-term beneficial effects, chronic adrenergic hyperactivation results in complex stimulation of signalling pathways eventually leading to deterioration of heart function [31]. This neurohormonal activation concomitant with the increased mechanical load makes *in vivo* models very complex systems with a huge matrix of variables to account for where separating the activation of molecular pathways due to hormonal stimulation from those of mechanical stimulation becomes extremely difficult. Basic science and intermediate models of myocardial physiology that can be studied *in vitro* but within a physiological environment of mechanical load and/or hormonal stimulation are the keys to understanding different and overlapping pathways of hormonal and mechanical systems and their interaction, and hold the promise for the development of much needed novel therapeutics.

References

1. Vincent JL (2008) Understanding cardiac output. Crit Care 12(4):174
2. Kumada M, Azuma T, Matsuda K (1967) The cardiac output-heart rate relationship under different conditions. Jpn J Physiol 17(5):538–555. [Internet] Available from: http://joi.jlc.jst.go.jp/JST.Journalarchive/jjphysiol1950/17.538?from=CrossRef
3. Wégria R, Frank CW, Wang H (1958) The effect of atrial and ventricular tachycardia on cardiac output, coronary blood flow and mean arterial pressure. Circ Res 6(5):624–632
4. Hamdani N, Kooij V, Van Dijk S, Merkus D, Paulus WJ, Dos RC et al (2008) Sarcomeric dysfunction in heart failure. Cardiovasc Res 77:649–658
5. Bers DM (2002) Cardiac excitation-contraction coupling. Nature 415:198–205
6. Sun YB, Irving M (2010) The molecular basis of the steep force-calcium relation in heart muscle. J Mol Cell Cardiol 48:859–865
7. Wiggers CJ (1951) Determinants of cardiac performance. Circulation 4(4):485–495
8. Levick JR (2009) An introduction to cardiovascular physiology, 5th edn. Hodder Arnold, London, pp 51–60
9. Bers DM (1991) Excitation-contraction coupling and cardiac contractile force. Springer, Netherlands
10. Allen DG, Kentish JC (1985) The cellular basis of the length-tension relation in cardiac muscle. J Mol Cell Cardiol 17:821–840
11. de Tombe PP, ter Keurs HEDJ (2016) Cardiac muscle mechanics: sarcomere length matters. J Mol Cell Cardiol 91:148–150
12. Fuchs F, Smith SH (2001) Calcium, cross-bridges, and the Frank-Starling relationship. News Physiol Sci 16(1):5–10. [Internet] Available from: http://physiologyonline.physiology.org/content/16/1/5.abstract
13. Solaro RJ (2007) Mechanisms of the Frank-Starling law of the heart: the beat goes on. Biophys J 93(12):4095–4096
14. Farman GP, Gore D, Allen E, Schoenfelt K, Irving TC, De Tombe PP (2011) Myosin head orientation: a structural determinant for the Frank-Starling relationship. Am J Physiol Heart Circ Physiol 300:2155–2160
15. Sonneblick HE, Downing SE (1963) Afterload as a primary determinant of ventricular performance. Am J Physiol Heart Circ Physiol 204:604–610
16. Nozawa T, Cheng CP, Noda T, Little WC (1994) Relation between left ventricular oxygen consumption and pressure-volume area in conscious dogs. Circulation 89(2):810–817
17. Suga H, Hayashi T, Shirahata M (1981) Ventricular systolic pressure-volume area as predictor of cardiac oxygen consumption. Am J Phys 240(1):H39–H44
18. Solaro RJ (2011) Regulation of cardiac contractility [internet]. In: Colloquium series on integrated systems physiology: from molecule to function, vol 3, pp 1–50. Available from: http://www.ncbi.nlm.nih.gov/books/NBK54078/
19. Florea VG, Cohn JN (2014) The autonomic nervous system and heart failure. Circ Res 114:1815–1826
20. Katz AM (1988) Influence of altered inotropy and lusitropy on ventricular pressure-volume loops. J Am Coll Cardiol 11(2):438–445
21. Suga H, Sagawa K, Shoukas AA (1973) Load independence of the instantaneous pressure-volume ratio of the canine left ventricle and effects of epinephrine and heart rate on the ratio. Circ Res 32:314
22. Ky B, French B, May Khan A, Plappert T, Wang A, Chirinos JA et al (2013) Ventricular-arterial coupling, remodeling, and prognosis in chronic heart failure. J Am Coll Cardiol 62:1165
23. Burkhoff D (2013) Pressure-volume loops in clinical research. J Am Coll Cardiol 62(13):1173–1176
24. Burchfield JS, Xie M, Hill JA (2013) Pathological ventricular remodeling: mechanisms: part 1 of 2. Circulation 128(4):388–400
25. Schotola H, Sossalla ST, Renner A, Gummert J, Danner BC, Schott P et al (2017) The contractile adaption to preload depends on the amount of afterload. ESC Hear Fail 4:468
26. Machackova J, Barta J, Dhalla NS (2006) Myofibrillar remodelling in cardiac hypertrophy, heart failure and cardiomyopathies. Can J Cardiol 22:953
27. Toischer K, Rokita AG, Unsöld B, Zhu W, Kararigas G, Sossalla S et al (2010) Differential cardiac remodeling in preload versus afterload. Circulation 122(10):993–1003

28. Drakos SG, Terrovitis JV, Anastasiou-Nana MI, Nanas JN (2007) Reverse remodeling during long-term mechanical unloading of the left ventricle. J Mol Cell Cardiol 43:231–242
29. Ibrahim M, Al Masri A, Navaratnarajah M, Siedlecka U, Soppa GK, Moshkov A et al (2010) Prolonged mechanical unloading affects cardiomyocyte excitation-contraction coupling, transverse-tubule structure, and the cell surface. FASEB J 24(9):3321–3329. [Internet] Available from: http://www.fasebj.org/cgi/doi/10.1096/fj.10-156638
30. Ibrahim M, Kukadia P, Siedlecka U, Cartledge JE, Navaratnarajah M, Tokar S et al (2012) Cardiomyocyte Ca2+handling and structure is regulated by degree and duration of mechanical load variation. J Cell Mol Med 16(12):2910–2918
31. Kishi T (2012) Heart failure as an autonomic nervous system dysfunction. J Cardiol 59:117–122
32. M. G. Hibberd, B. R. Jewell, (1982) Calcium- and length-dependent force production in rat ventricular muscle. The Journal of Physiology 329 (1):527-540